A 5 ps TOF-counter with an MCP-PMT

K. Inami, N. Kishimoto, Y. Enari, M. Nagamine, T. Ohshima
Department of Physics, Nagoya University, Chikusa, Nagoya 464-8602, Japan

1. Introduction

With a time-of-flight (TOF) resolution of $\sigma_{\rm TOF} < 10$ ps, K/π separation of more than 4σ could be attained up to $p \simeq 4$ GeV/c in the case of a flight path-length of $L \sim 1$ m. This performance could provide an excellent and simple particle identification for medium-energy particles in experiments in, for instance, a B-factory. A micro-channel plate (MCP) photo-multiplier tube (PMT) generally provides good timing resolution. The transit time spread of $\sigma_{\rm TTS}$ is $30-40$ ps [1].

A TOF counter has exhibited $\sigma_{\rm TOF} = 10.6$ ps at a beam-test, as reported in our previous paper [1], while it was predominated by the readout circuit uncertainty of $\sigma_{\rm circuit} = 7-9$ ps. In the case of an MCP-PMT alone irradiated by a pion beam under normal conditions, the detected number of photo-electrons, $\rm N_{p.e.}$, was twice as that of the expected value; it was inferred to be produced from the first MCP layer.

In order to examine this inference and the achievable timing resolution of a TOF counter with an ineffectual $\sigma_{\rm circuit}$ contribution, we at this time employed a readout electronics module of $\sigma_{\rm circuit} = 4$ ps and carried out a beam-test at KEK-PS using 3 GeV/c pions. Some results are here reported and discussed.

2. TOF counters and a Readout Module

Two TOF counters were prepared in the same way as the previous ones (see, Fig.1), but the MCP-PMT's were Hamamatsu (HPK) 3809U-50-11X instead of the previous HPK 3809U-50-25X, to which we hereafter refer to as HPK6 and HPK10, respectively. The essential difference between the two MCP-PMT's was the channel diameter: The former had D = 6 μm, resulting in $\sigma_{\rm TTS} \simeq 30$ ps, while the latter had D = 10 μm and $\sigma_{\rm TTS} \simeq 40$ ps. Also, as an important parameter in this study, the window was made of 3 mm-thick quartz rather than 4 mm, as in the previous one. The characteristics of the MCP-PMT's can be found in ref.[1] and are listed in Table 1. The quartz radiator of 10 mm$^{\phi}$ was attached in front of the MCP-PMT, as in the previous case, but its thickness was varied instead of the previous 40 mm-thick one. We express the total quartz length, a sum of the radiator length and the window of 3 mm-thick, by ℓ in mm.

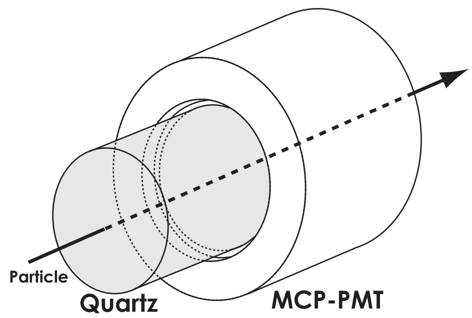

Fig. 1. Schematic drawing of the TOF counter

Figure 2(a) illustrates the setup for the beam test. 3 GeV/c negative pion beam was prepared with the following properties: It had a size of a few cm$^{\phi}$, a momentum spread of $\sim \pm 1$ %, and an intensity of $\sim$10 Hz with a negligible electron contamination. The TOF counters described above were separated by 30 cm along the beam line. Trigger counters with scintillators of

Table 1
Characteristics of HPK6 and HPK10. Both PMT's are of two-stage type with the single-anode. The fourth raw indicates the distance from the photo-cathode to MCP, the thickness of MCP plates, and the distance from the MCP to anode.

MCP-PMT	HPK6	HPK10
diameter of MCP-PMT (mm)	45^{ϕ}	52^{ϕ}
diameter of effective size (mm)	11^{ϕ}	25^{ϕ}
photo-cathode	multi-alkali	multi-alkali
gaps (mm)	2.1 / 0.03 / 1.0	1.1 / 0.03 / 0.94
D ♮ (μm)	6	10
α = L/D ♮	40	43
bias angle (^{o})	13	12
max. voltage (kV)	3.6	3.6
voltage-divider ratio	2 : 4 : 1	2 : 4 : 1
gain	2×10^6	4×10^5

♮ D and L are the diameter and length of the MCP plate, respectively, and α = L/D.

$5\mathrm{mm}^W \times 5\mathrm{mm}^H \times 10\mathrm{mm}^t$ defined the beam position.

The readout electronics was the time-correlated single-photon counting module (SPC-134), Becker & Hickl GmbH's, that exhibits a channel resolution of 813 fs, a time resolution of 4 ps in rms, and repetition rates up to 200 MHz. Our system was composed of 4 modules, each of them comprising constant fraction discriminators (CFD), a time-to-amplitude converter (TAC), an ADC and a multi-channel analyzer (MCA).

The output signals of the TOF counters were directly fed to SPC modules, as illustrated in Fig. 2(b). A coincidence between the two trigger counters was prepared to give a stop timing signal for the SPC's. We took a difference between TDC outputs of the two TOF counters in the analysis, so that timing fluctuation of the stop signal was ineffective.

3. Performance of MCP-PMT

The performance of HPK6 was measured using single-photons from a light pulser. Figures 3(a) and (b) show the output signals and TDC distribution, respectively. The HV dependences of TTS, gain (G) and photo-electron collection efficiency (CE) can be seen in (c), (d) and (e), respectively. The HPK6's used exhibited $\sigma_{\mathrm{TTS}} = 32{-}33$ ps with G$\geq 10^6$.

HV of 3.4 kV was applied on the both TOF counters during the beam test.

4. Beam Test

4.1. Timing resolutions

Figure 4(a) shows the output signals of the TOF counter for 3 GeV/c pions. An ADC vs TDC scatter plot is shown in (b): CFD functioned so as to keep the TDC distribution flat regardless of the ADC size.

Figure 5(a) is for the TOF counters with 10 mm-thick quartz radiator, and (b) is without a radiator. Each provided $\sigma_{\mathrm{TOF}} = 6.2$ ps and 7.7 ps, respectively. Fig. 5(c) shows the SPC module resolution obtained by feeding the same signals into the start and stop modules: $\sigma_{\mathrm{circuit}} = 4.1$ ps. The TOF counter therefore exhibited its intrinsic timing resolution of $\sigma_{\mathrm{TOF}} = 4.7$ ps ($= \sqrt{6.2^2 - 4.1^2}$) with ℓ = 13 mm, and 6.5 ps without radiator ($\ell = 3$).

4.2. ℓ dependence of σ_{TOF} and $N_{\mathrm{p.e.}}$

$N_{\mathrm{p.e.}}$ and σ_{TOF} were measured by changing the quartz thickness, as plotted in Fig. 6(a) and (b), respectively, where open circles indicate results of a Monte-Carlo simulation. GEANT program was used in the Monte-Carlo simulation to consider

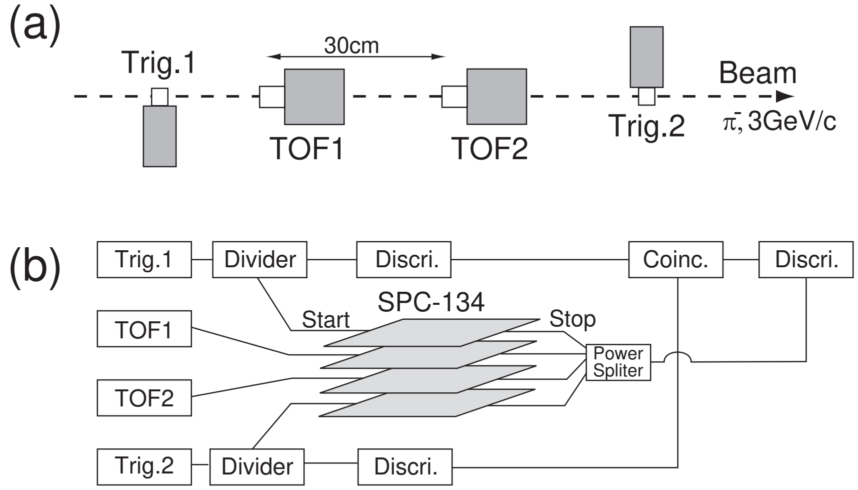

Fig. 2. (a) Setup of the beam test, and (b) Configuration of readout electronics

interactions of pions with the quartz; Cherenkov radiations by the beam-pions and charged particles, including δ-rays, resulted from GEANT were next simulated in our program as well as their propagation in the quartz and the PMT performance.

$N_{\rm p.e.}$ was evaluated by comparing the signal amplitudes to that of the single-photons. Since HPK6 has a quartz window of 3 mm-thickness, $N_{\rm p.e.}$ is expected to be $\sim$20 at $\ell = 3$ mm, while it was measured as $\sim$70-80. The same as the previous measurement, we observe extra photo-electrons again.

A large difference could be seen between the measured and expected $N_{\rm p.e.}$'s. There are two ways to read the data. One is that both $N_{\rm p.e.}$'s have the same gradient of $\sim$ 50 p.e./10 mm, but the measured one has $\sim 70-80$ larger amounts. This number, $N_{\rm p.e.} \sim$ 50 p.e./10 mm, is consistent with our previous study. The another reading is that $N_{\rm p.e.}$/10 mm becomes slightly larger when ℓ is narrower.

The best resolution, $\sigma_{\rm TOF}$ = 6.2 ps, was attained with ℓ = 13 mm, and at $\ell >$ 13 mm $\sigma_{\rm TOF}$ deteriorated with ℓ, even though $N_{\rm p.e.}$ increased. This was because the arrival time spread of the Cherenkov photons became influential with a larger ℓ.

4.3. Extra photo-electrons from the first MCP-layer

By irradiating the counters with the pion beam, we supplied the same high-voltage on both the photo-cathode and the first MCP layer, so that the photo-electrons from the photo-cathode could not be accelerated and, resultantly, could not have sufficient energy to produce secondaries even though they arrived at the first MCP layer. Therefore, the primary photo-electrons emitted from the photo-cathode were suppressed, and only the extra photo-electrons could be detected if they were produced downstream of the photo-cathode, probably at the first MCP-layer. Figure 7 is the observed ADC distribution; $N_{\rm p.e.} \sim$ 1. It suggests that the extra photo-electrons did not originate from the MCP-layer, but were produced upstream of the photo-cathode: Our previous inference is not the right solution.

5. Discussion and Summary

Some remarks made below require further studies.

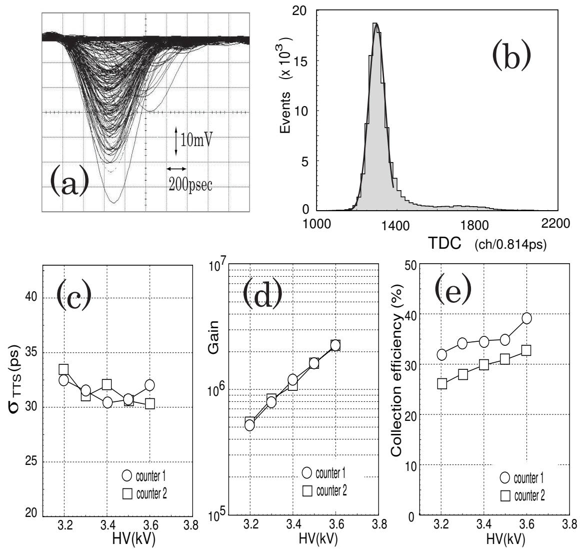

Fig. 3. Performance of the HPK6, measured using single-photons.

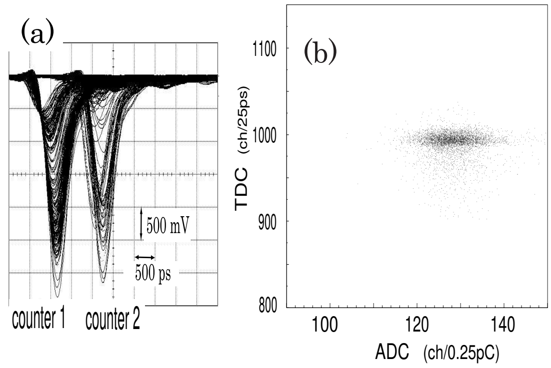

Fig. 4. Signals of 3 GeV/c pion beams. (a) Output signals of two TOF counters, and (b) their TDC vs ADC scatter plots are shown.

Extra photo-electrons:

Fig. 7 shows the observed numbers of photo-electrons at every 10 mm of quartz by closed circles and the expected ones by open circles. As in the previous observation, in the case of an MCP-PMT alone, we obtained larger amounts than expected: It was about 4-times, but not twice, larger. The observed $N_{\rm p.e.}/10$ mm sharply decreased with an ~ 10 mm attenuation length, and coincided with the expected numbers at $\ell > 23$ mm. If the extra photo-electrons were really produced by Cherenkov light as well as the expected number of photo-electrons were, the time resolutions could be much improved: It is expected to be 5-6 ps and 5 ps at $\ell = 3$ mm and 13 mm, respectively, including $\sigma_{\rm circuit} = 4.1$ ps, as described below. Our data disagree with this.

We do not understand the reason for the time being. However, we infer that the extra photo-electrons were actually produced, but did not have a timing spread narrow enough to improve the time resolution, nor wide enough to appear at the signal shape.

Radiator thickness effect:

The beam particles passed the quartz at almost the light velocity, c, while Cherenkov light was radiated at nearly 45^o from the beam and traveled with a velocity c/n (n = refraction index = 1.47 for quartz). Therefore, the arrival time difference between the light emitted at the entrance and at the exit of the quartz was approximately ℓ/c. The emitted Cherenkov light was uniformly distributed over this time interval, so that the statistical timing fluctuation of all light was

$$\sigma_\ell \sim \frac{\ell/c}{\sqrt{12}\sqrt{N_{\rm p.e.}}} \tag{1}$$

$$= \frac{30\ ({\rm ps/cm}) \times \ell}{\sqrt{12}\sqrt{(40-50)\ell}} \sim 1.3\sqrt{\ell}\ ({\rm ps}), \tag{2}$$

where the expected relation $N_{\rm p.e.} = (40-50)\ell$ is assumed with ℓ in units of cm.

$\sigma_{\rm TOF}$ is composed of σ_ℓ and the two other contributions. One is attributed to the TTS fluctuation, and is approximated to be

$$\sigma_{\rm MCP} \sim \sigma_{\rm TTS}/\sqrt{N_{\rm p.e.}} \tag{3}$$

$$\sim \frac{5}{\sqrt{\ell}}\ ({\rm ps}), \tag{4}$$

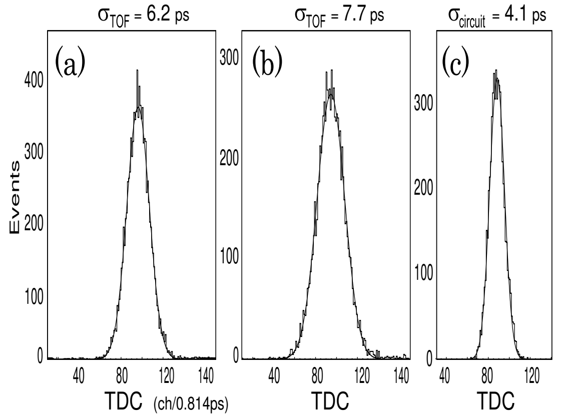

Fig. 5. TOF resolutions obtained using 3 GeV/c pion beams. (a) is with a 10 mm-thick quartz radiator and (b) is without a radiator. (c) is the SPC module resolution.

where $\sigma_{\mathrm{TTS}} = 33$ ps is applied. The other is

$$\sigma_{\mathrm{circuit}} \simeq 4.1 \text{ (ps)}. \tag{5}$$

σ_{TOF}, expressed as σ_{cal} below, was calculated by adding the above three contributions in quadrature:

$$\sigma_{\mathrm{cal}} \sim \sqrt{1.7\ell + \frac{25}{\ell} + 16.8}. \tag{6}$$

This simple approximation resulted in a similar value to that obtained by a Monte-Carlo simulation. While the latter additionally included the direct interactions of pions with the quartz window, they were not likely to be the origin of this discrepancy since the quartz window of 3 mm-thick is only 2.4 % and 0.68 % in terms of the radiation length and nuclear interaction length, respectively.

Figure 8(b) plots σ_{cal} and their components of σ_ℓ and σ_{MCP}.

It is obvious that the deterioration of σ_{TOF} at $\ell > 23$ mm cannot be reproduced in our simple explanation. Data rapidly deteriorate faster than the expectation. The extra photo-electrons may take a considerable portion of the observed $N_{\mathrm{p.e.}}$,

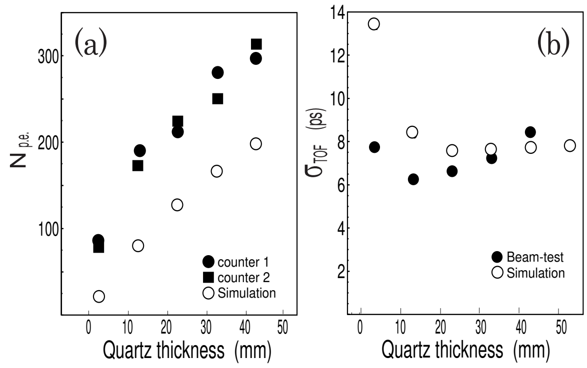

Fig. 6. $N_{\mathrm{p.e.}}$ and σ_{TOF} dependence on the quartz thickness. Closed and open circles are of observed data and by Monte-Carlo simulation.

not only at $\ell < 23$ mm, but also at $\ell > 23$ mm, so that σ_ℓ would predominate σ_{TOF}.

In summary, our TOF counter achieved $\sigma_{\mathrm{TOF}} = 6.2$ ps, or its intrinsic resolution of 4.7 ps by subtracting the readout electronics uncertainty. This indicates a possible way to attain a high TOF resolution of around 5 ps, although there still exists, for us, an issue that requires further studies.

Acknowledgments

This work is supported by a Grant-in-Aid for Science Research on Priority Area (Mass Origin and Supersymmetry Physics) from the Ministry of Education, Culture, Sports, Science and Technology of Japan.

REFERENCES

1. M. Akatsu *et al.*, Nucl. Instr. and Meth. **A 528** (2004) 763-775.
2. Y. Enari *et al.*, Nucl. Instr. and Meth. **A 547** (2005) 490-503.

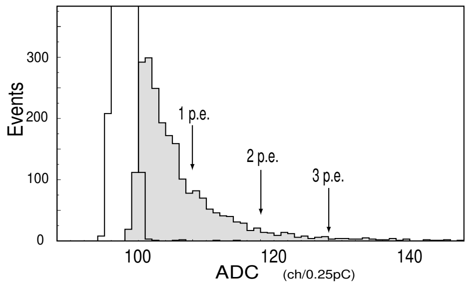

Fig. 7. ADC distribution, obtained by applying the same high-voltage on the photo-cathode and the first MCP layer. The offset is at 100-th channel, and a pedestal distribution is indicated by an open histogram. The peak channels of 1, 2 and 3 photo-electrons distributions are indicated, based on the single-photons calibration.

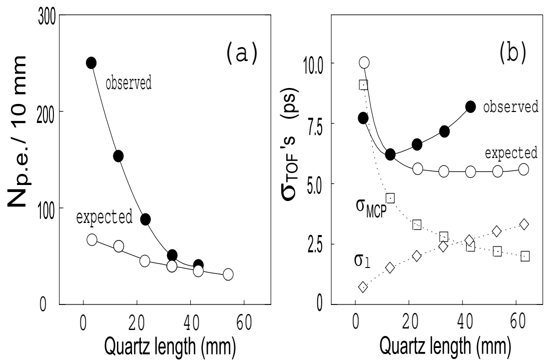

Fig. 8. Observed and expected $N_{\mathrm{p.e.}}/10$ mm (a) and σ_{TOF} (b) as a function of ℓ. The σ_ℓ of eq.(2), and σ_{MCP} of eq.(4) are plotted in (b).